PHYSICAL REVIEW B VOLUME 46, NUMBER 9 1 SEPTEMBER 1992-I

Domain-array melting in the dipolar lattice gas

M. M. Hurley and Sherwin J. Singer
Department of Chemistry, Ohio State University, Columbus, Ohio 43210
(Received 10 January 1992)

A lattice gas with long-range R^{-3} repulsive interactions is shown to support disk and stripe domains, as well as complex intermediate domain structures. In a sharp-interface limit we examine melting of two-dimensional crystals of disk domains, and the analogous destruction of the stripe phase driven by changing density and temperature. The stripe phase provides an example of a material with two-dimensional smectic order.

The interplay of attractive and repulsive forces plays a key role in self-organization processes in ferromagnetic thin films,[1,2] Langmuir monolayers,[3-7] surfactant micelles,[8,9] and membranes.[10] The two-dimensional dipolar lattice gas, with competing nearest-neighbor attractions and long-range dipolar repulsions, furnishes a simple model for self-organization phenomena:

$$\mathcal{H}=-J\sum_{\langle \mathbf{R},\mathbf{R}'\rangle} n_{\mathbf{R}}n_{\mathbf{R}'}+\frac{A}{2}\sum_{\mathbf{R},\mathbf{R}'}{}' \frac{n_{\mathbf{R}}n_{\mathbf{R}'}}{|\mathbf{R}-\mathbf{R}'|^3}-\mu\sum_{\mathbf{R}} n_{\mathbf{R}} \ . \tag{1}$$

The R^{-3} dipolar repulsion is chosen to mimic the long-range interactions in thin ferromagnetic films and Langmuir monolayers. The occupation variables $n_{\mathbf{R}}$ of lattice site $\mathbf{R}$ take the values 0 or 1 for the lattice gas (or ± 1 for the isomorphic spin lattice model).

There is a considerable body of literature on dipolar continua.[1,2,4,6] The Monte Carlo studies reported here begin the elucidation of the behavior of a microscopic model, the dipolar lattice gas, as a function of temperature (J^{-1}) and relative repulsion strength ($\eta \equiv A/J$). From our previously reported results for the zero-temperature phase diagram of the dipolar lattice gas[11] the low-temperature equilibrium domain structure is known as a function of η and fractional coverage ρ. The studies reported here show that the equilibrium domain morphology is far richer than considered in previous work.[12] Simulations of systems as large as 15 776 spins indicate that the equilibrium phase diagram differs from the mean-field phase diagram[2,6] at the value of repulsion strength η used in our simulations. Of course, from numerical evidence alone we cannot exclude the possibility that further increase in the system size will alter our results.

The periodically replicated simulation cell in most of our work contains 3944 spins taken from a rectangular (nearly square) area of the triangular spin lattice. In one case we increased the system size to 15 776 spins. The computations are demanding for several reasons: the simulation cell is relatively large; a long-range interaction with all other spins, not just nearest neighbors, must be calculated for each attempted spin flip; and long runs are needed to equilibrate the system for certain values of J, η, and μ. We found Metropolis Monte Carlo sampling was enhanced by adding multiple spin flips and by concentrating attempted moves near domain interfaces.[13] The interaction potential is calculated by two-dimensional Ewald summation. The specific value of $\eta=\frac{3}{7}$ was chosen so a typical domain size would be a suitable fraction of the simulation cell dimension. The combination of parameters studied in this work lies in a sharp interface limit in which we can study ordering and melting of arrays of well-defined domains.

The dipolar lattice gas supports disk and stripe domain phases (Fig. 1), as well as more complicated domain textures. We are concerned with translational and orientational ordering of the domains into superlattices. The m-fold symmetry of these phases was quantified by the order parameter

$$f_m \equiv \sum_{\mathbf{k}} \exp(im\phi_{\mathbf{k}})S(\mathbf{k}) \ , \tag{2}$$

where $S(\mathbf{k})$ is the structure factor and the sum over $\mathbf{k}$ extends over the set of reciprocal lattice vectors for the

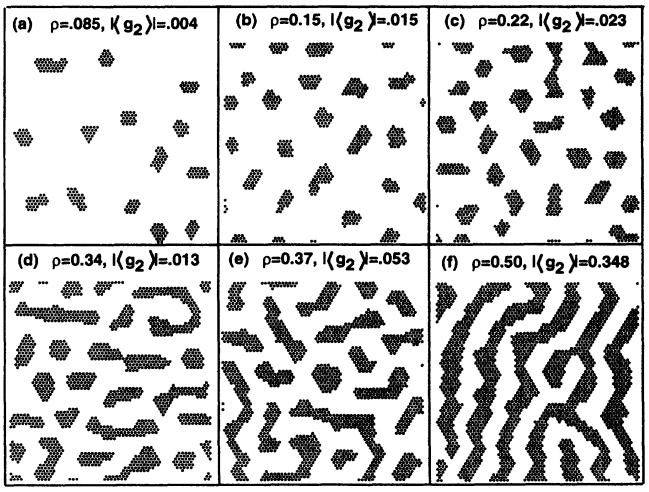

FIG. 1. Instantaneous configurations at several values of the chemical potential μ, and with $J=9.5$, $\eta=\frac{3}{7}$. The average coverage and orientational order parameter g_2 [Eq. (3)] are shown next to each figure.

periodic system. Twofold stripe order was also quantified by a more conveniently accumulated order parameter that signals long-range interfacial orientational correlation:

$$g_2 \equiv \sum_{\langle \mathbf{R},\mathbf{R}' \rangle} \exp(2i\theta_{\mathbf{R},\mathbf{R}'})[n_{\mathbf{R}}(1-n_{\mathbf{R}'})+(1-n_{\mathbf{R}})n_{\mathbf{R}'}] . \tag{3}$$

The sum extends over all nearest-neighbor pairs on the lattice. The combination of occupation variables in square brackets identifies those bond pairs at an interface, and $\theta_{\mathbf{R},\mathbf{R}'}$ is the angle between the normal to that interface (along the vector $\mathbf{R}-\mathbf{R}'$) and a reference direction.

The stripe domain phase is an example of a material with two-dimensional smectic order. There has been interest in phase transitions,[14] and the topological[15,16] and dynamical[17] properties of defects in two-dimensional smectics. This work is the first demonstration of which we are aware of a microscopic model exhibiting two-dimensional smectic order. It is well known that fluctuations cause algebraic decay of translational and orientational correlations with distance in two-dimensional crystals. Two-dimensional smectics are characterized by exponential decay of translational order and algebraic decay of orientational order at low temperatures.[14] Order parameters with slowly decaying correlations show up as full long-range order in simulations with periodic boundary conditions. The special role of fluctuations in two dimensions, even near zero temperature, must be borne in mind when applying our results for a periodically replicated finite system to a truly infinite material.

A constant temperature cut in the ρ-T phase plane at $J=9.5$ reveals a progression of domain morphologies shown in Fig. 1. Isolated lattice-gas monomers coalesce into faceted disk domains [Fig. 1(a)] at very low density. As density increases, the disk domains elongate [Figs. 1(b) and 1(c)], and the snakelike domains [Figs. 1(d) and 1(e)] also seen experimentally in epifluorescence microscopy appear.[18] Eventually the elongated domains form a stripe phase [Fig. 1(f)], as quantified by the orientational order parameter g_2.

From the configurations in Figs. 1(a) and 1(b), it is not apparent whether the disk phase exhibits hexagonal order of a two-dimensional supercrystal of disk domains. According to the mean-field phase diagram[2,6] we should encounter isotropic-to-hexagonal and hexagonal-to-stripe transitions as the density is increased at this temperature. We sought a definitive answer to this question by lowering the temperature at $\rho \approx 0.15$ and monitoring the sixfold order parameter f_6 for the location of an isotropic-hexagonal phase boundary. If crystallization were observed, it would confirm that the configurations shown in Figs. 1(a) and 2(b) were isotropic. At densities much much above ~ 0.15 the question of whether disk domains form a two-dimensional solid rapidly loses meaning as the domains elongate.

Unfortunately, spin flips become increasingly rare at low temperatures and ordinary Monte Carlo sampling is not practical for J much greater than 9.5. We did obtain information about the low temperature disk phase by

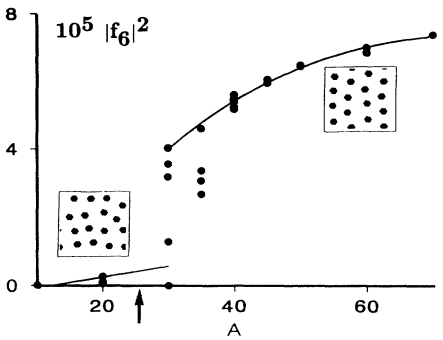

FIG. 2. Sixfold order parameter [Eq. (2)] of a system of 16 hexagonal domains as a function of repulsion strength A. (See text for further explanation.) An arrow marks the point where a continuous system of particles with similar R^{-3} interactions melt (Refs. 19 and 20). The insets show typical disordered and ordered configurations.

freezing certain degrees of freedom that would tend to disrupt the solid, thereby establishing an upper limit for the isotropic-hexagonal boundary. We investigated a system of perfect hexagonal domains with density $\rho \approx 0.15$ (see insets to Fig. 2). These frozen disk systems can be simulated at low temperatures just like off-lattice particles. Freezing domain shape fluctuations only enhances crystalline order and drives the freezing temperature to a higher value than the original lattice model. A system of 16 faceted hexagonal disks, each containing 37 particles, produces an almost perfect triangular domain crystal within our simulation cell with density $\rho=0.1501$ (Fig. 2). Only the repulsion term controlled by the parameter $A=J\eta$ plays a role in the frozen-domain studies because nearest-neighbor interaction energy is constant unless two domains come into contact, which is very unlikely.

The hexagonal order parameter f_6 for frozen disk domain as a function of A is shown in Fig. 2. Crystalline order arises in the range $30 < A < 40$. This implies that $70 < J < 90$ provides an upper limit to the freezing temperature at $\eta=\frac{3}{7}$ and $\rho \approx 0.15$. Our lattice results are supported by available data for two-dimensional continuous particle systems interacting with a pair potential, $v(r)=\epsilon(\sigma/r)^3$,[19,20] characterized by one dimensionless parameter $\Gamma=\beta\epsilon\sigma^3(\pi\rho')^{3/2}$. Here ρ' corresponds to *domains* per unit area. The continuous system freezes at $\Gamma_f \approx 62$.[19,20] Associating the domains of Fig. 2 with a continuous system on the basis of the long-range interaction between domains (which is purely r^{-3}),[11] we would expect $A_f \approx 25.4$ from the continuous system results. The comparison with our frozen lattice domain calculations is reasonable, given the inherent differences between continuous and lattice systems, and supports our contention that hexagonal disk domain order is *not* present in the $J=9.5$ systems of Fig. 1. It is unlikely that disk domains will crystallize with increasing density before the disklike morphology is completely lost for reasons discussed below.

A transition between the isotropic and stripe phase can be driven by temperature as well as density. The sequence of $\rho=\frac{1}{2}$, variable J configurations in Fig. 3 clearly shows that the twofold stripe order is lost while the

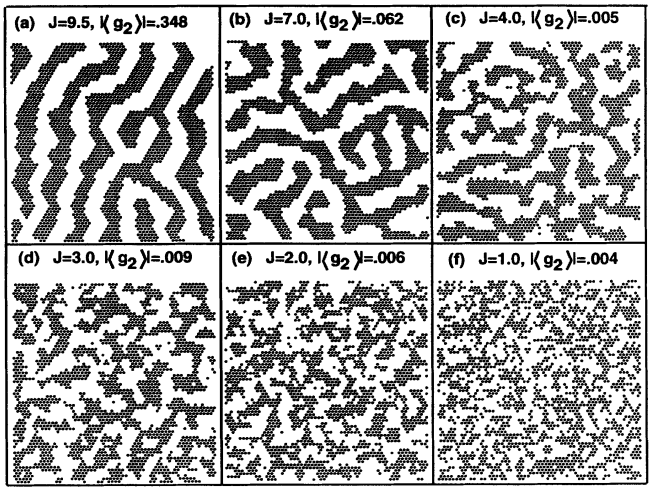

FIG. 3. Instantaneous configurations at several values of the inverse temperature J at $\rho=\frac{1}{2}$. The average order parameter g_2 [Eq. (3)] for each run is shown next to the representative configuration.

domain interface is still sharp. In other words, the stripe melting temperature at $\eta=\frac{3}{7}$ is found to be far below the critical point, $J_c=1.10$, of the lattice gas without repulsions.[21] At $J=7.5$ stripe order as measured by g_2 is clearly absent. Stripe order appears to be fixed at $J=9.0$, providing a lower limit for the freezing temperature. At this temperature the system spontaneously orders and remains ordered (Fig. 4). Because of limitations on system size and equilibration times, it is not presently feasible to determine the stripe melting point with greater precision. We did check for system size dependence in a system of 15 776 spins initialized as a stripe array at $J=9.0$. The stripe order was stable for the length of the run (Fig. 4), $\sim 10^4$ attempted moves per spin or 1.7×10^8 total attempted moves on the larger system.

Our conjectured phase diagram for $\eta=\frac{3}{7}$, which falls in the Brazovskiĭ class,[22] is shown in Fig. 5. The dashed line is an estimated upper limit to the isotropic-hexagonal boundary obtained by assuming that the transition temperature scales with density as would the continuous system of particles with R^{-3} repulsive interactions,

$$\frac{1}{J}\propto[n_{\mathcal{D}}(\rho)]^{1/2}\rho^{3/2}\ . \tag{4}$$

We have incorporated the fact that the equilibrium domain size $n_{\mathcal{D}}$ will be a function of density, and used the domain size of faceted hexagonal domains at zero temperature to estimate this dependence.[11] Note that the dashed line in Fig. 5 does not reach the stripe melting region ($J\sim 9$) until almost half-coverage. By this point the disklike domain morphology is completely lost (Fig. 1). The isotropic-hexagonal-stripe triple points are only conjectured, and we cannot exclude other possibilities, such as elongation of disk domains disrupting the solid, forcing an isotropic region to intervene between hexagonal

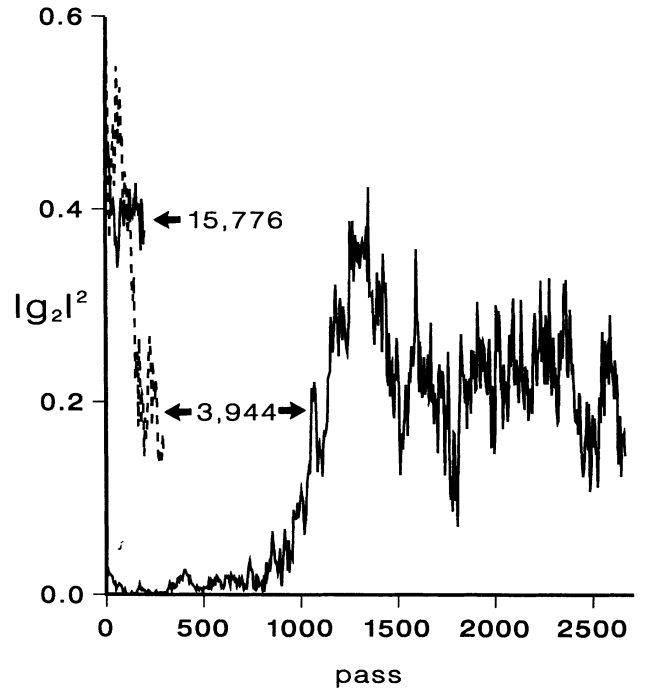

FIG. 4. Evolution of stripe order parameter g_2 [Eq. (3)] as a function of the number of Monte Carlo passes through the system (Ref. 13) at $J=9.0$. Each pass involves 54 attempted moves per spin (Ref. 13.) A solid and dashed line shows $|g_2|^2$ for 3944 particles, initialized in a completely disordered high-temperature configuration in a perfect stripe array, respectively. Another solid line shows the evolution of a very large 15 776 spin system during $\sim 10^4$ attempted moves per spin after initialization as perfect stripes.

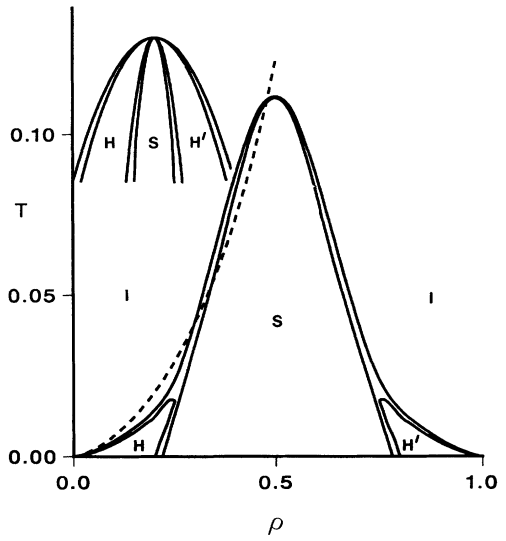

FIG. 5. Phase diagram for the dipolar lattice gas appropriate near $\eta=\frac{3}{7}$, the shape interface limit studied in this work (**I**=isotropic, **H**=hexagonal, **H′**=inverted hexagonal, **S**=stripe). For comparison, the mean-field phase diagram is shown in the upper left. The **H-S** and **H′-S** boundaries at zero temperature were established in previous work (Ref. 11.) The height of the stripe phase region and the direct **I-S** transition with no intervening **H** or **H′** phases are results of this work. The **I-H-S** and **I-H′-S** triple points are conjectured. The dashed line indicates an upper limit to the **I-H** boundary based on scaling of particles with R^{-3} interactions [Eq. (4)].

and stripe phases, or long-range orientational order of elongated domains. It has been proposed that loss of orientational order in two-dimensional smectic materials occurs when dislocations (whose presence does not destroy orientational order) unbind into disclination pairs.[14] Testing the applicability of this mechanism to stripe melting in the dipolar lattice gas will be left to future work. The structures observed during stripe melting are also highly reminiscent of those found in the "labyrinthine" phase of ferromagnetic thin films.[1,23]

[1]C. Kittel, Phys. Rev. **70**, 965 (1946); C. Kooy and U. Enz, Philips Res. Rep. **15**, 7 (1960); A. A. Thiele, J. Appl. Phys. **41**, 1139 (1970); W. A. Barker and G. A. Gehring, J. Phys. C **16**, 6415 (1983); R. E. Rosensweig, M. Zahn, and R. Shumovich, J. Magn. Magn. Mater. **39**, 127 (1983); D. Sornette, J. Phys. **48**, 151, (1987); **48**, 1413 (1987).

[2]T. Garel and S. Doniach, Phys. Rev. B **26**, 325 (1982).

[3]C. M. Knobler, Adv. Chem. Phys. **77**, 397 (1990).

[4]H. M. McConnell, Annu. Rev. Phys. Chem. **42**, 171 (1991).

[5]H. Möhwald, in *Phase Transitions in Soft Condensed Matter,* edited by T. Riste and D. Sherrington (Plenum, New York, 1989), p. 145.

[6]D. Andelman, F. Broçhard, and J.-F. Joanny, J. Chem. Phys. **86**, 3673 (1987).

[7]M. Seul and M. J. Sammon, Phys. Rev. Lett. **64**, 1903 (1990).

[8]C. Tanford, *The Hydrophobic Effect: Formation of Micelles and Biological Aggregates* (Wiley, New York, 1980).

[9]S. W. Haan and L. R. Pratt, Chem. Phys. Lett. **79**, 436 (1981); B. Owenson and L. R. Pratt, J. Phys. Chem. **88**, 2905 (1984); L. R. Pratt, B. Owenson, and Z. Sun, Adv. Colloid Interface Sci. **26**, 69 (1986).

[10]O. G. Mouritsen, in *Physics of Living Matter,* Springer Lectures Notes in Physics, Vol. 284, edited by D. Baeriswyl, M. Droz, A. Malaspinas, and P. Martinoli (Springer, New York, 1987), p. 76; J. Charvolin, in *Soft Condensed Matter,* edited by T. Riste and D. Sherrington, (Plenum, New York, 1989), p. 95.

[11]M. M. Hurley and S. J. Singer, J. Phys. Chem. **96**, 1938 (1992); **96**, 1951 (1992).

[12]Recent dynamical simulations of a continuum model by R. Desai and co-workers also exhibit complex domain morphologies. See C. Roland and R. C. Desai, Phys. Rev. B **42**, 6658 (1990); R. C. Desai, C. Sagui, and K. R. Elder, *Structure and Dynamics of Supramolecular Aggregates and Strongly Interacting Colloids,* Vol. 369 of *NATO Advanced Study Institute, Series C: Mathematical and Physical Sciences* edited by S. H. Chen, J. S. Huang, and P. Tartaglia (Kluwer Academic, Boston 1992), p. 205.

[13]Each "pass" through the system of N spin lattice sites consisted of N attempted flips of randomly chosen spins, N attempted flips of triangles of three spins, another N attempted single spin flips, N attempted flips of hexagons of 7 spins, and $50N$ attempts to flip spins located at a domain interface. The interfacial moves greatly increase the acceptance rate because the overwhelming majority of attempted moves in the interior of a domain are rejected in a strong interface limit.

[14]J. Toner and D. R. Nelson, Phys. Rev. B **23**, 316 (1981).

[15]V. Poénaru and G. Toulouse, J. Phys. (Paris) **38**, 887 (1977).

[16]N. D. Mermin, Rev. Mod. Phys. **51**, 591 (1979).

[17]S. Ostlund, J. Toner, and A. Zippelius, Ann. Phys. (N.Y.) **144**, 345 (1982).

[18]Our simulations should be compared to the experimentally observed domain morphologies shown in Fig. 3 of W. M. Heckl and H. Möhwald, Ber. Bunsenges. Phys. Chem. **90**, 1159 (1986).

[19]R. K. Kalia and P. Vashishta, J. Phys. C **14**, L643 (1981).

[20]V. M. Bedanov, G. V. Gadiyak, and Y. E. Lozovik, Phys. Lett. **92A**, 400 (1982).

[21]The critical value of J quoted here is four times the usual value, since our J is defined by the lattice gas Hamiltonian in Eq. (1).

[22]S. A. Brazovksiĭ, Zh. Eksp. Teor. Fiz. **68**, 175 (1975) [Sov. Phys. JETP **41**, 85 (1975)].

[23]P. Molho, J. Gouzerh, J. C. S. Levy, and J. L. Porteseil, J. Magn. Magn. Mater. **54-57**, 857 (1986); P. Molho, J. L. Porteseil, Y. Souche, J. Gouzerh, and J. C. S. Levy, J. Appl. Phys. **61**, 4188 (1987).

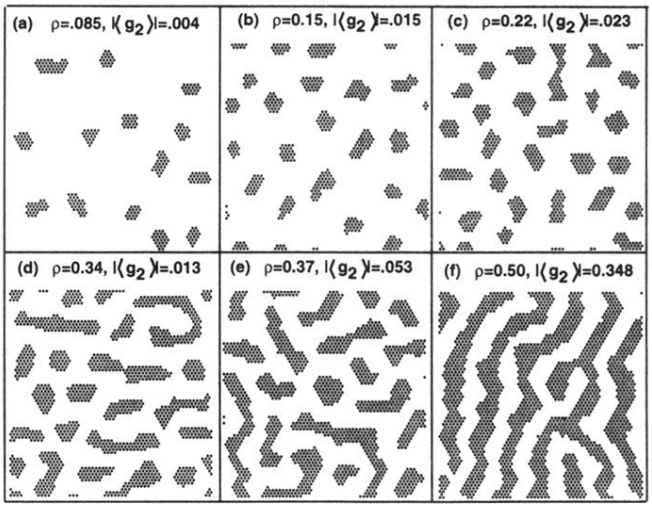

FIG. 1. Instantaneous configurations at several values of the chemical potential μ, and with $J=9.5$, $\eta=\frac{3}{7}$. The average coverage and orientational order parameter g_2 [Eq. (3)] are shown next to each figure.

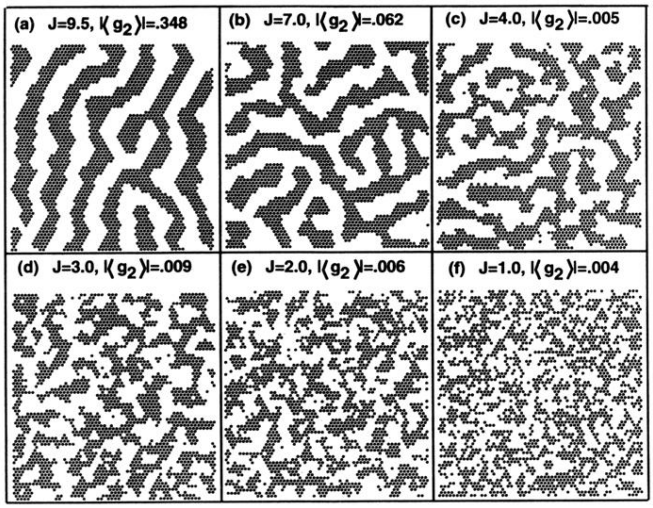

FIG. 3. Instantaneous configurations at several values of the inverse temperature J at $\rho=\frac{1}{2}$. The average order parameter g_2 [Eq. (3)] for each run is shown next to the representative configuration.